Hydrogen Production Hot Paper

DOI: 10.1002/ange.201408266

A Molecular Copper Catalyst for Electrochemical Water Reduction with a Large Hydrogen-Generation Rate Constant in Aqueous Solution**

Peili Zhang, Mei Wang, Yong Yang, Tianyi Yao, and Licheng Sun*

Abstract: *The copper complex [(bztpen)Cu](BF$_4$)$_2$ (bztpen = N-benzyl-N,N′,N′-tris(pyridin-2-ylmethyl)ethylenediamine) displays high catalytic activity for electrochemical proton reduction in acidic aqueous solutions, with a calculated hydrogen-generation rate constant (k_{obs}) of over 10000 s^{-1}. A turnover frequency (TOF) of 7000 h^{-1} cm^{-2} and a Faradaic efficiency of 96% were obtained from a controlled potential electrolysis (CPE) experiment with [(bztpen)Cu]$^{2+}$ in pH 2.5 buffer solution at −0.90 V versus the standard hydrogen electrode (SHE) over two hours using a glassy carbon electrode. A mechanism involving two proton-coupled reduction steps was proposed for the dihydrogen generation reaction catalyzed by [(bztpen)Cu]$^{2+}$.*

The availability of electric energy directly generated from renewable energy sources, such as sunlight, wind, and tides, is often inconsistent with the temporal fluctuation and the geographic distribution of energy demand. One of the practical and promising technologies for the efficient storage of surplus electric energy is to use it for the electrolytic conversion of water into hydrogen, and the reverse hydrogen combustion reaction can regenerate energy when and where it is needed, for example, through the use of fuel cells. This energy storage and regeneration cycle is a clean process that does not release carbon dioxide or other pollutants. For this purpose, the key issue is to reduce the catalyst cost and enhance the energy conversion efficiency by developing catalysts that comprise only earth-abundant elements and display high activities with low overpotentials and good stabilities for electrolysis of water. In recent years, a number of molecular iron,[1–4] cobalt,[5–11] nickel,[12,13] and molybdenum complexes[14,15] have been shown to be electrocatalytically active for hydrogen generation in fully aqueous solutions at onset overpotentials from 80 to 740 mV and display high Faradaic efficiencies.[16–19]

Copper complexes with a well-defined coordination chemistry and diverse redox chemistry have attracted extensive attention and have been used as catalysts for various transformations. To our surprise, to date no copper complex has been reported to be an active catalyst for water reduction to hydrogen either in organic media or in aqueous solutions, although some copper complexes have been used for CO_2 reduction[20] and very recently for water oxidation.[21–24] Herein we report an ionic copper complex featuring a diamine-tripyridine ligand, which displays a high catalytic activity ($k_{obs} > 10000\ s^{-1}$) with a 420 mV onset overpotential and 96% Faradaic efficiency in acidic aqueous solutions. To the best of our knowledge, this is the first example of a homogeneous copper electrocatalyst for water reduction.

The mononuclear copper complex [(bztpen)Cu](BF$_4$)$_2$ (bztpen = *N*-benzyl-*N*,*N*′,*N*′-tris(pyridin-2-ylmethyl)ethylenediamine) was conveniently prepared from the reaction of Cu(BF$_4$)$_2$·6H$_2$O with the bztpen ligand in water (see the Supporting Information). The product [(bztpen)Cu](BF$_4$)$_2$ was obtained as a light-blue crystalline solid in 89% yield. The high-resolution mass spectrometry (HR-MS) and elemental analysis data of the product are in good agreement with the proposed composition of [(bztpen)Cu](BF$_4$)$_2$. The single-crystal structure (Figure 1) confirmed that the bztpen acted as a pentadentate ligand in [(bztpen)Cu](BF$_4$)$_2$. The pyridine (Py) of the N(CH$_2$Py)(CH$_2$Ph) unit in bztpen is coordinated at an apex, which is opposite to an axial amine nitrogen atom bonding to two 2-pyridylmethyl groups. The copper(II) center resides in a distorted trigonal-bipyramidal geometry.[25] In [(bztpen)Cu]$^{2+}$, the axial bond, Cu–N5

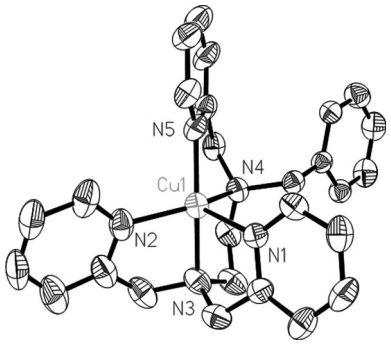

Figure 1. Molecular structure of [(bztpen)Cu](BF$_4$)$_2$. Counterions, solvent molecules, and hydrogen atoms are omitted for clarity; thermal ellipsoids set at 30% probability.

[*] P. Zhang, Prof. M. Wang, Y. Yang, T. Yao, Prof. L. Sun
State Key Laboratory of Fine Chemicals, DUT-KTH Joint Education and Research Center on Molecular Devices
Dalian University of Technology (DUT)
116024 Dalian (China)
E-mail: symbueno@dlut.edu.cn
Prof. L. Sun
Department of Chemistry, KTH Royal Institute of Technology
10044 Stockholm (Sweden)

[**] This work was supported by the Natural Science Foundation of China (21373040, 21120102036, 21361130020, and 91233201), the Basic Research Program of China (2014CB239402), the Ph.D. Program Foundation of the Ministry of Education of China (20130041110024), the Swedish Research Council, the Swedish Energy Agency, and the K & A Wallenberg Foundation.

Supporting information for this article is available on the WWW under http://dx.doi.org/10.1002/anie.201408266.

(1.988(5) Å), is apparently shorter than the Cu–N(Py) bonds (2.130(5) and 2.014(5) Å) in the equatorial plane, and the Cu–N3 axial bond (2.033(5) Å) is also slightly shorter than the Cu–N4(amine) bond (2.080(5) Å) owing to Jahn–Teller effects.

The cyclic voltammogram (CV) of $[(bztpen)Cu](BF_4)_2$ in acetonitrile (Figure 2) displays a reversible redox event at $E_{1/2} = +0.10$ V (all potentials given in this paper are versus the standard hydrogen electrode (SHE)), which was assigned to a metal-based Cu^{II}/Cu^{I} reduction, and a quasi-reversible reduction event at $E_{1/2} = -0.59$ V, corresponding to a Cu^{I}/Cu^{0} redox process. The differential pulse voltammogram (DPV)

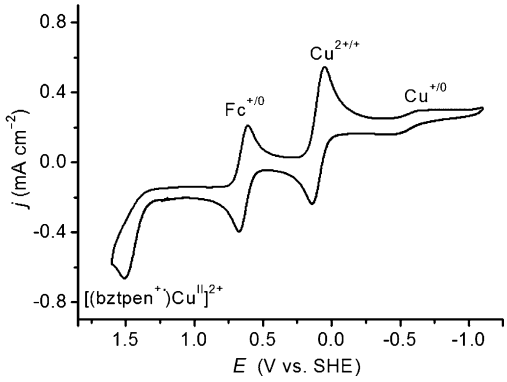

Figure 2. Cyclic voltammogram of $[(bztpen)Cu](BF_4)_2$ (1.0 mM) in Bu_4NPF_6 acetonitrile solution (0.1 M) with an internal reference ($E_{1/2}$ ($Fc^{+/0}$) = 0.64 V vs. SHE; Fc = ferrocene), using a 0.07 cm^2 glassy carbon electrode at a scan rate of 100 $mV s^{-1}$.

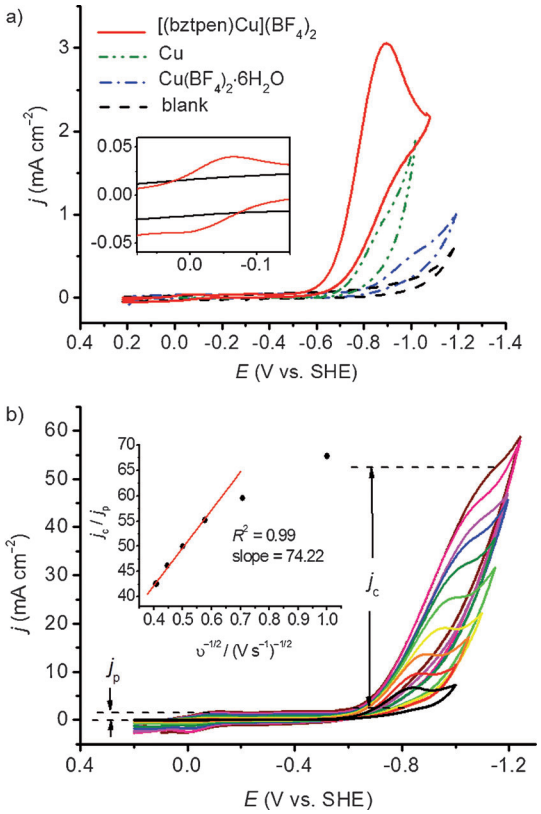

Figure 3. a) Cyclic voltammograms of $[(bztpen)Cu](BF_4)_2$ (0.5 mM; red) and $Cu(BF_4)_2 \cdot 6H_2O$ (0.5 mM; blue); the blank CVs of a copper plate electrode (green) and a glassy carbon electrode (black) in 0.1 M phosphate buffer at pH 2.5 under N_2 atmosphere at a scan rate of 50 $mV s^{-1}$ are also shown. Inset: Enlarged view of the reversible reduction wave at −0.03 V. b) Cyclic voltammograms of $[(bztpen)Cu](BF_4)_2$ (0.5 mM) at various scan rates from 0.05 to 6.00 $V s^{-1}$. Inset: plot of j_c/j_p versus the reciprocal of the square root of scan rate.

of $[(bztpen)Cu](BF_4)_2$ exhibited two reduction peaks at +0.11 and −0.62 V under the same conditions (Supporting Information, Figure S1 a), which are consistent with the reduction waves in the CV. The assignment of these two reduction waves to the copper-centered reduction processes is further supported by the fact that the free bztpen ligand and the analogous cobalt and nickel complexes $[(bztpen)M(CH_3CN)](BF_4)_2$ (M = Co, Ni) are all electrochemically silent in the range of +0.5 to −0.75 V (Figure S2).[10,13] With anodic scanning, an irreversible oxidation peak at +1.29 V is attributed to a ligand-based one-electron oxidation process of $[(bztpen)Cu^{II}]^{2+}$ to $[(bztpen^{+\cdot})Cu^{II}]^{2+}$. Accordingly, the CV of the free ligand, bztpen, in an acetonitrile solution containing Bu_4NPF_6 (0.1 M) displayed an irreversible oxidation peak at +1.00 V.

The cyclic voltammetry experiments with $[(bztpen)Cu](BF_4)_2$ and $Cu(BF_4)_2 \cdot 6H_2O$ were carried out in phosphate buffers at pH 2.5 with a glassy carbon disc as the working electrode. The $Cu(BF_4)_2 \cdot 6H_2O$ salt displayed a tardy increase in current arising at −0.85 V (Figure 3 a). In contrast, $[(bztpen)Cu](BF_4)_2$ exhibited a reversible redox peak corresponding to the Cu^{II}/Cu^{I} couple at $E_{1/2} = -0.03$ V (Figure 3 a, inset) and a proton reduction catalytic peak arising sharply at −0.57 V, corresponding to an onset overpotential of 420 mV. The onset of catalytic current observed for $[(bztpen)Cu](BF_4)_2$ is approximately 280 mV more positive than that of the $Cu(BF_4)_2$ salt under identical conditions. The catalytic current increased with a negative shift of the potential, with a peak value of −0.87 V, and the evolution of gas bubbles was observed from the electrode surface. The H_2 evolved was detected by GC analysis. A value of $j_c/j_p = 77$ was measured at a scan rate of 50 $mV s^{-1}$, indicating the high activity of $[(bztpen)Cu]^{2+}$ for electrochemical H_2 generation. The DPV of $[(bztpen)Cu](BF_4)_2$ (Figure S1 b) in a pH 2.5 phosphate buffer shows a reduction peak at −0.03 V for the Cu^{II}/Cu^{I} couple and a catalytic peak at −0.82 V, similar to the reduction events visible in Figure 3 a. As shown in Figures S3 and S4, the redox peak current of Cu^{II}/Cu^{I} displays a linear relation to the square root of the scan rate, which was varied from 0.05 to 1.0 $V s^{-1}$, and the current also increases linearly with an increase in the concentration of $[(bztpen)Cu](BF_4)_2$, indicating that the copper complex functions in a diffusion-controlled regime under the test conditions, and that it is a molecular catalyst in nature. Furthermore, the linear relation shown in the plot of the current density maximum against the square root of the H_3O^+ concentration shows that hydrogen generation is also first order in the H_3O^+ concentration (Figure S5).[26]

The following equation [Eq. (1)], which was established

$$\frac{j_c}{j_p} = \frac{2}{0.446}\sqrt{\frac{RTk_{obs}}{Fv}} \quad (1)$$

on the basis of an approximate model for a first-order or pseudo-first-order H_2 evolving reaction that is catalyzed by freely diffusing molecular catalysts,[27–30] is often used to estimate the apparent rate constant (k_{obs}) for electrocatalytic H_2 evolution.[31–34] Sometimes, the use of this equation was extended to estimate catalytic rates of systems working according to more complicated or undetermined catalytic mechanisms.[6,7,21]

In Eq. (1), j_c is the maximum current density of the catalytic peak, j_p is the plateau current density of the noncatalytic wave (here taken from the reversible reduction wave of the Cu^{II}/Cu^{I} couple), R is the universal gas constant, T is the temperature in Kelvin, F is Faraday's constant, v is the scan rate, and k_{obs} is the observed first-order rate constant.

The electrocatalytic activity of $[(bztpen)Cu](BF_4)_2$ was estimated by plotting j_c/j_p as a function of $v^{-1/2}$. The CV of $[(bztpen)Cu](BF_4)_2$ (Figure 3b) shows that j_c only slightly increased at a scan rate faster than 3 $V s^{-1}$, and a plot of j_c/j_p as a function of $v^{-1/2}$ is linear at high scan rates ($v \geq 3$ $V s^{-1}$). The k_{obs} value, calculated from the slope (74.22) of a fit line (Figure 3b, inset) according to Eq. (1), is over 10000 s^{-1} in aqueous solution at pH 2.5 at 20 °C. This rate constant is significantly higher than those reported to date for molecular non-noble-metal electrocatalysts working in fully aqueous solutions and approximately 33 and 13 times larger than the corresponding k_{obs} values reported for cobalt tetraaza macrocycles (295 s^{-1}) in pH 2.2 buffer solution[7] and for a bis(iminopyridine) cobalt complex (700 s^{-1}) in pH 4 buffer solution,[6] respectively. The highest j_c/j_p (74) and k_{obs} (106000 s^{-1}) values thus far reported were observed for $[Ni(P^{Ph}_2N^{Ph})_2](BF_4)_2$ ($P^{Ph}_2N^{Ph}$ = 1,3,6-triphenyl-1-aza-3,6-diphosphacycloheptane) in an organic medium, namely acetonitrile, containing [(DMF)H]OTf (0.43 M; Tf = trifluoromethanesulfonyl) and a small amount of water.[31]

Controlled potential electrolysis (CPE) experiments with $[(bztpen)Cu](BF_4)_2$ in 0.1 M phosphate buffer solution at pH 2.5 were conducted at −0.90 V with a 2.0 cm^2 large glassy carbon plate as the working electrode for 30 minutes to estimate the Faradaic efficiency for H_2 production catalyzed by $[(bztpen)Cu]^{2+}$. A comparison of the amount of H_2 detected by GC analysis and that calculated from the consumed charge in the CPE experiment shows that $[(bztpen)Cu]^{2+}$ electrochemically catalyzes H_2 generation with a Faradaic efficiency of approximately 96% (Figure S6).

Extended CPE experiments with $[(bztpen)Cu](BF_4)_2$ were conducted at various applied potentials in pH 2.5 buffer solutions for two hours (Figure 4). A total of 300 C of charges was passed during the electrolysis at −0.90 V, corresponding to a turnover number (TON) of 1.4×10^4 mol H_2 (mol cat)$^{-1}$ cm^{-2} and a turnover frequency (TOF) of 7000 mol H_2 (mol cat)$^{-1}$ h^{-1} cm^{-2}. The TONs of H_2 evolution calculated on the basis of the cumulated charge and the Faradaic efficiency are 9600 at −0.8 V, 5800 at −0.7 V, and 2900 mol H_2 (mol cat)$^{-1}$ cm^{-2} at −0.6 V for a two-hour electrolytic process, corresponding to TOFs of 4800, 2900, and 1450 mol H_2 (mol cat)$^{-1}$ h^{-1} cm^{-2}, respectively (Table S3).

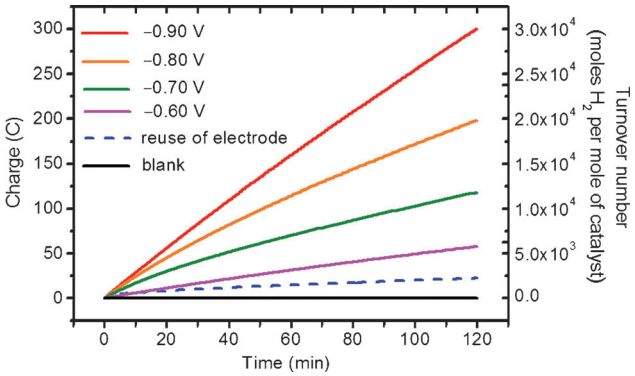

Figure 4. Extended controlled potential electrolysis of $[(bztpen)Cu](BF_4)_2$ (5.0 μM) in 0.1 M phosphate buffer at pH 2.5 with $NaBF_4$ (0.1 M) as a supporting electrolyte, showing cumulative charge over time for various applied potentials from −0.90 to −0.60 V over 120 minutes and the control experiment in the absence of catalyst at −0.90 V (black); after electrolysis with $[(bztpen)Cu](BF_4)_2$ for 120 minutes at −0.90 V, the working electrode was thoroughly rinsed with distilled water, and the controlled potential electrolysis was repeated using a freshly made pH 2.5 buffer solution in the absence of catalyst at −0.90 V (blue).

These values are the lower limits of the TON and TOF as 1) the CPE experiments were carried out without Ohmic internal resistance compensation, and 2) the calculations were made by using the number of catalyst molecules in the entire bulk solution, whereas only the small fraction of catalyst molecules that interact with the electrode are contributing to H_2 production. Nevertheless, all catalytic data show that $[(bztpen)Cu]^{2+}$ is a highly active catalyst for electrochemical H_2 production from acidic water. It is difficult to directly compare the electrocatalytic activities of diverse molecular electrocatalysts, as the electrolysis experiments made in different laboratories differ in the conditions used, such as the type of the reaction cell, the electrode area, the applied potential, the pH value, as well as the types and concentrations of electrolyte, buffer, and acid source in the aqueous solution. Among the recently reported non-noble-metal-based molecular catalysts, the most efficient ones that display TOF values of more than 100 mol H_2 (mol cat)$^{-1}$ h^{-1} cm^{-2} for electrochemical H_2 production from water are a molybdenum oxo pentapyridine complex that displays a TOF of 434 mol H_2 (mol cat)$^{-1}$ h^{-1} cm^{-2} at −1.40 V (71 h) in 3.0 M phosphate buffer at pH 7,[14] a cobalt tripyridine-diimine complex that affords a TOF of 860 mol H_2 (mol cat)$^{-1}$ h^{-1} cm^{-2} at −1.25 V (60 h) in 2.0 M phosphate buffer at pH 7,[10] a self-assembled cobalt complex CoP_4N_2 that exhibits a TOF of 1490 mol H_2 (mol cat)$^{-1}$ h^{-1} cm^{-2} at −1.0 V (20 h) in 2.0 M phosphate buffer at pH 7,[11] and a side-on-bound molybdenum disulfide pentapyridine complex that gives an upper-limit TOF value of 4.2×10^4 mol H_2 (mol cat)$^{-1}$ h^{-1} cm^{-2} (calculated by assuming that a monolayer of catalyst molecules is adsorbed on the surface of the Hg electrode) at −0.96 V (23 h) in 3.0 M aqueous acetate buffer at pH 3.[15] It is noticeable that all of these high TOF values were obtained for bulk electrolysis reactions with molecular catalysts and a mercury electrode, whereas the TOF value of

7000 mol H_2 (mol cat)$^{-1}$ h^{-1} cm^{-2} for the electrolysis catalyzed by $[(bztpen)Cu]^{2+}$ at −0.90 V was obtained using a glassy carbon electrode, which is a scalable and environmentally benign electrode.

To determine whether the catalytically active species was deposited onto the surface of the working electrode after controlled-potential bulk electrolysis with $[(bztpen)Cu](BF_4)_2$ in a pH 2.5 phosphate buffer at −0.90 V over two hours, the working electrode was thoroughly rinsed with distilled water, and the electrode was reused for the CPE experiment in the absence of catalyst under otherwise identical conditions. A value of 22.1 C of charges was cumulated during the two-hour electrolytic process (blue dashed line in Figure 4) with a Faradaic efficiency of approximately 94% (Figure S7). SEM and EDX analysis (Figure S8) of the surface of the used working electrode indicate a slight electrodeposition of the molecular copper catalyst during bulk electrolysis for two hours under the applied conditions, but the electrochemical H_2 evolution reaction is dominantly catalyzed by the complex $[(bztpen)Cu]^{2+}$. The electronic absorbance spectrum of $[(bztpen)Cu](BF_4)_2$ in water shows two intense ligand $\pi\rightarrow\pi^*$ absorptions at $\lambda_{max}=258$ and 290 nm (Figure S9a), together with a weak broad absorption at $\lambda_{max}\approx700$ nm, which is attributed to Cu^{II} d–d transitions (Figure S9a, inset). Monitoring of the electrolysis process by UV/Vis spectroscopy showed that the intensity of the ligand absorption of $[(bztpen)Cu]^{2+}$ at 258 nm had decreased by approximately 8% after two hours of electrolysis in a pH 2.5 aqueous solution at −0.90 V (Figure S9b), indicating that the concentration of the Cu^{II} complex remains high in the bulk solution. This spectroscopic evidence is consistent with the results obtained from SEM and EDX analysis and from the CPE experiments.

Further DPV, CV, UV/Vis, and ^{1}H NMR spectroscopic studies provided additional information on the mechanism of the H_2 evolving reaction catalyzed by $[(bztpen)Cu]^{2+}$. The Pourbaix diagrams (Figure S10 and S11) show that the reduction potential of the Cu^{II}/Cu^{I} wave and the potential of the catalytic peak both shift linearly with the pH value in the pH range of 1.9–4.0, with a slope of −53 and −60 mV per pH unit, respectively. These observations are indicative of one electron reduction coupled by one proton in each reduction process. On the basis of this evidence, two possible pathways were proposed. The key difference between these two pathways is that for pathway A [Eqs. (2) and (3)], protonation takes place at the Cu^{I} center in the first step, whereas for pathway B [Eqs. (4)–(6)], protonation occurs at one of the nitrogen atoms of the ligand.

Proposed pathway A:

$$[(bztpen)Cu^{II}]^{2+} + e^- + H^+ \xrightarrow{-0.03\ V} [(bztpen)Cu^{III}(H)]^{2+} \quad (2)$$

$$[(bztpen)Cu^{III}(H)]^{2+} + e^- + H^+ \xrightarrow{-0.85\ V} [(bztpen)Cu^{II}]^{2+} + H_2 \quad (3)$$

Proposed pathway B:

$$[(bztpen)Cu^{II}]^{2+} + e^- + H^+ \xrightarrow{-0.03\ V} [(bztpen)Cu^{I}]^{2+} \quad (4)$$

$$[(bztpen)Cu^{I}]^{2+} + e^- + H^+ \xrightarrow{-0.85\ V} [(bztpen)Cu^{II}(H)]^{2+} \quad (5)$$

$$[(bztpen)Cu^{II}(H)]^{2+} \rightarrow [(bztpen)Cu^{III}]^{2+} + H_2 \quad (6)$$

A UV/Vis–SEC (SEC = spectroelectrochemical) spectroscopic study of $[(bztpen)Cu](BF_4)_2$ was carried out in water at −0.3 V. At such a low applied potential, only the first steps of pathway A and B can take place, and the second step cannot be driven. The intensity of the ligand absorption at $\lambda_{max}=258$ nm gradually decreased while the absorption at 290 nm simultaneously increased during the reduction of $[(bztpen)Cu]^{2+}$ at −0.3 V (Figure S12), accompanied with the appearance of a new band at $\lambda_{max}=350$ nm, which was assigned to the one-electron-reduced species of $[(bztpen)Cu]^{2+}$. The decrease in intensity of the broad absorption at $\lambda_{max}=700$ nm and the fading of the blue color of the solution support the formation of the Cu^{I} species; the apparent changes in the UV absorption spectrum of the ligand implicate that the coordination mode of the ligand in the Cu^{I} species has changed significantly compared to the Cu^{II} complex.

To gain further insight into the structure of the Cu^{I} species generated in the copper-catalyzed H_2 generation reaction, an analogous Cu^{I} complex was prepared from the reaction of $[Cu(CH_3CN)_4](BF_4)$ with the bztpen ligand in CH_3CN and characterized by mass spectrometry and ^{1}H and ^{13}C NMR as well as UV/Vis spectroscopy (see the Supporting Information). The broad absorption of the ligand of $[(bztpen)Cu]^{+}$ at 340 nm in water (Figure S9a) is similar to the new band attributed to the Cu^{I} species in the UV/Vis–SEC spectra of $[(bztpen)Cu](BF_4)_2$ (Figure S12).

The ^{1}H NMR spectrum of $[(bztpen)Cu]^{+}$ displays two characteristic signals at chemical shifts greater than $\delta=8.0$ ppm (Figure S13a), one at $\delta=9.09$ ppm (d, 1H) and the other one at $\delta=8.41$ ppm (d, 2H). The former Py signal shifts downfield by 0.67 ppm compared to the corresponding signal of the free bztpen ligand, representing an *ortho* hydrogen atom of the Py coordinated to the Cu^{I} center, whereas the chemical shift of the latter Py signal is very similar to that of the free ligand, which was ascribed to the *ortho* hydrogen atoms of the other two equivalent Py units in the ligand. The remarkable broadening of the signal of the Py *ortho* hydrogen atoms at $\delta=8.41$ ppm in the variable-temperature ^{1}H NMR spectra of $[Cu(bztpen)](BF_4)$ indicates a fast association/dissociation equilibrium for the two equivalent pyridine units in solution at room temperature (Figure S14a). Such an association/dissociation equilibrium of a Cu^{I} amine-pyridine complex has been reported in the literature.[35] A comparison of the chemical shifts for the methylene protons of the free bztpen ligand and $[(bztpen)Cu](BF_4)$ at $\delta=2.5$–4.0 ppm (Figure S13b) shows that the two amine moieties of the ligand are coordinated to the Cu^{I} center in solution, whereas the broadening of these methylene signals in the variable-temperature ^{1}H NMR spectra (Figure S14b) of $[Cu(bztpen)](BF_4)$ suggests that fluxional processes associated with the methylene units occur. According to these spectroscopic observations, we assume that in the Cu^{I} complex containing a bztpen ligand, one pyridine and two amine units are coordinated, and the other two equivalent pyridine moieties

are in a fast association/dissociation equilibrium. The dissociated Py unit should have precedence over the copper center for the protonation in the first proton-coupled reduction step of the mechanism, leading to a $[(bztpenH)Cu^{I}]^{2+}$ intermediate according to pathway B. The further proton-coupled catalytic reduction process may result in the formation of a $[(bztpenH)Cu^{II}(H)]^{2+}$ copper hydride species, which could release H_2 and regenerate the catalyst in its initial form, $[(bztpen)Cu]^{2+}$, to close the catalytic cycle. The assumed formation of the intermediate $[bztpenH)Cu(H)]^{2+}$ is consistent with the CV (Figure S5 a) and DPV (Figure S10 a) data obtained at various pH values, which clearly indicate that two successive proton-coupled reduction processes occur in the electrocatalytic H_2 generation reaction catalyzed by $[(bztpen)Cu]^{2+}$ in acidic water. Monitoring of the further $[(bztpen)Cu](BF_4)$ reduction process by UV/Vis–SEC spectroscopy did not provide any useful information on the mechanism because of the poor stability of $[(bztpen)Cu]^{+}$ in water.

In conclusion, the ionic copper complex $[(bztpen)Cu]^{2+}$, which contains an amine-pyridine-based pentadentate ligand with five coordinating nitrogen atoms, displayed a hydrogen-generation rate constant (k_{obs}) of over $10000\,s^{-1}$ with a 420 mV onset overpotential in buffer solution at pH 2.5. The controlled potential electrolysis of $[(bztpen)Cu](BF_4)_2$ in a pH 2.5 phosphate buffer at −0.90 V over two hours using a glassy carbon electrode gave a TON of $1.4\times10^4\,mol\,H_2\,(mol\,cat)^{-1}\,cm^{-2}$ with a Faradaic efficiency of approximately 96%, which corresponds to a TOF of approximately $2.0\,mol\,H_2\,(mol\,cat)^{-1}\,s^{-1}\,cm^{-2}$. This electrochemical water reduction reaction is predominantly catalyzed by a molecular copper catalyst in a diffusion-controlled regime under our test conditions. The results obtained from electrochemical and spectroscopic studies support that the H_2 generation reaction takes place by two successive proton-coupled reduction processes, with protonation occurring at the ligand in the first reduction step and at the Cu^{I} center in the second step to afford a $[(bztpenH)Cu^{II}(H)]^{2+}$ copper hydride species, which could release H_2 and regenerate the Cu^{II} catalyst in its initial form. The results presented here provide an opportunity for the development of highly efficient copper-based catalysts for electrochemical water reduction. Further studies on the mechanism of this process and on further copper complexes for water reduction are in progress in our laboratory.

Received: August 15, 2014
Published online: October 14, 2014

Keywords: copper · electrocatalysis · hydrogen · water reduction

[1] R. Mejia-Rodriguez, D. Chong, J. H. Reibenspies, M. P. Soriaga, M. Y. Darensbourg, *J. Am. Chem. Soc.* **2004**, *126*, 12004 – 12014.
[2] Y. Na, M. Wang, K. Jin, R. Zhang, L. Sun, *J. Organomet. Chem.* **2006**, *691*, 5045 – 5051.
[3] M. L. Singleton, J. H. Reibenspies, M. Y. Darensbourg, *J. Am. Chem. Soc.* **2010**, *132*, 8870 – 8871.
[4] F. Quentel, G. Passard, F. Gloaguen, *Energy Environ. Sci.* **2012**, *5*, 7757 – 7761.
[5] Y. Sun, J. P. Bigi, N. A. Piro, M. L. Tang, J. R. Long, C. J. Chang, *J. Am. Chem. Soc.* **2011**, *133*, 9212 – 9215.
[6] B. D. Stubbert, J. C. Peters, H. B. Gray, *J. Am. Chem. Soc.* **2011**, *133*, 18070 – 18073.
[7] C. L. C. McCrory, C. Uyeda, J. C. Peters, *J. Am. Chem. Soc.* **2012**, *134*, 3164 – 3170.
[8] W. M. Singh, T. Baine, S. Kudo, S. Tian, X. A. N. Ma, H. Zhou, N. J. DeYonker, T. C. Pham, J. C. Bollinger, D. L. Baker, B. Yan, C. E. Webster, X. Zhao, *Angew. Chem. Int. Ed.* **2012**, *51*, 5941 – 5944; *Angew. Chem.* **2012**, *124*, 6043 – 6046.
[9] Y. Sun, J. Sun, J. R. Long, P. Yang, C. J. Chang, *Chem. Sci.* **2013**, *4*, 118 – 124.
[10] P. Zhang, F. Gloaguen, F. Quentel, *Chem. Commun.* **2013**, *49*, 9455 – 9457.
[11] L. Chen, M. Wang, K. Han, P. Zhang, F. Gloaguen, L. Sun, *Energy Environ. Sci.* **2014**, *7*, 329 – 334.
[12] O. R. Luca, S. J. Konezny, J. D. Blakemore, D. M. Colosi, S. Saha, G. W. Brudvig, V. S. Batista, R. H. Crabtree, *New J. Chem.* **2012**, *36*, 1149 – 1152.
[13] P. Zhang, Y. Yang, D. Zheng, Han, *Chem. Commun.* **2014**, DOI: 10.1039/C4CC05511J.
[14] H. I. Karunadasa, C. J. Chang, J. R. Long, *Nature* **2010**, *464*, 1329 – 1333.
[15] H. I. Karunadasa, E. Montalvo, Y. Sun, M. Majda, J. R. Long, C. J. Chang, *Science* **2012**, *335*, 698 – 702.
[16] V. Artero, M. Chavarot-Kerlidou, M. Fontecave, *Angew. Chem. Int. Ed.* **2011**, *50*, 7238 – 7266; *Angew. Chem.* **2011**, *123*, 7376 – 7405.
[17] P. Du, R. Eisenberg, *Energy Environ. Sci.* **2012**, *5*, 6012 – 6021.
[18] M. Wang, L. Chen, L. Sun, *Energy Environ. Sci.* **2012**, *5*, 6763 – 6778.
[19] V. S. Thoi, Y. Sun, J. R. Long, C. J. Chang, *Chem. Soc. Rev.* **2013**, *42*, 2388 – 2400.
[20] R. Angamuthu, P. Byers, M. Lutz, A. L. Spek, E. Bouwman, *Science* **2010**, *327*, 313 – 315.
[21] S. M. Barnett, K. I. Goldberg, J. M. Mayer, *Nat. Chem.* **2012**, *4*, 498 – 502.
[22] Z. Chen, T. J. Meyer, *Angew. Chem. Int. Ed.* **2013**, *52*, 700 – 703; *Angew. Chem.* **2013**, *125*, 728 – 731.
[23] M. Zhang, Z. Chen, P. Kang, T. J. Meyer, *J. Am. Chem. Soc.* **2013**, *135*, 2048 – 2051.
[24] T. Zhang, C. Wang, S. Liu, J. Wang, W. Lin, *J. Am. Chem. Soc.* **2014**, *136*, 273 – 281.
[25] P. Kumar, A. Kalita, B. Mondal, *Dalton Trans.* **2013**, *42*, 5731 – 5739.
[26] A. J. Bard, L. R. Faulkner, *Electrochemical Methods: Fundamentals and Applications*, 2ednd edWiley, New York, **2001**.
[27] J. M. Saveant, E. Vianello, *Electrochim. Acta* **1965**, *10*, 905 – 920.
[28] J. M. Savéant, E. Vianello, *Electrochim. Acta* **1967**, *12*, 629 – 646.
[29] C. P. Andrieux, J. M. Dumas-Bouchiat, J. M. Saveant, *J. Electroanal. Chem.* **1980**, *113*, 1 – 18.
[30] J. M. Savéant, *Chem. Rev.* **2008**, *108*, 2348 – 2378.
[31] L. M. Helm, M. P. Stewart, R. M. Bullock, M. R. DuBois, D. L. DuBois, *Science* **2011**, *333*, 863 – 866.
[32] U. J. Kilgore, J. A. S. Roberts, D. H. Pool, A. M. Appel, M. P. Stewart, M. R. DuBois, W. G. Dougherty, W. S. Kassel, R. M. Bullock, D. L. DuBois, *J. Am. Chem. Soc.* **2012**, *134*, 3164 – 3170.
[33] D. H. Pool, M. P. Stewart, M. O'Hagan, W. J. Shaw, J. A. S. Roberts, R. M. Bullock, D. L. DuBois, *Proc. Natl. Acad. Sci. USA* **2012**, *109*, 15617 – 15621.
[34] X. Hu, B. S. Brunschwig, J. C. Peters, *J. Am. Chem. Soc.* **2007**, *129*, 8988 – 8998.
[35] H. Tang, N. Arulsamy, M. Radosz, Y. Shen, N. V. Tsarevsky, W. A. Braunecker, W. Tang, K. Matyjaszewski, *J. Am. Chem. Soc.* **2006**, *128*, 16277 – 16285.

